

# The quantum interference effect transistor

Charles A Stafford<sup>1</sup>, David M Cardamone<sup>2</sup> and Sumit Mazumdar<sup>1</sup>

<sup>1</sup> Department of Physics, University of Arizona, 1118 E. 4th Street, Tucson, AZ 85721, USA

<sup>2</sup> Department of Physics, Simon Fraser University, 8888 University Drive, Burnaby, BC, V5A 1S6, Canada

E-mail: [stafford@physics.arizona.edu](mailto:stafford@physics.arizona.edu)

Received 3 May 2007, in final form 25 July 2007

Published 13 September 2007

Online at [stacks.iop.org/Nano/18/424014](http://stacks.iop.org/Nano/18/424014)

## Abstract

We give a detailed discussion of the quantum interference effect transistor (QuiET), a proposed device which exploits the interference between electron paths through aromatic molecules to modulate the current flow. In the off state, perfect destructive interference stemming from the molecular symmetry blocks the current, while in the on state, the current is allowed to flow by locally introducing either decoherence or elastic scattering. Details of a model calculation demonstrating the efficacy of the QuiET are presented, and various fabrication scenarios are proposed, including the possibility of using conducting polymers to connect the QuiET with multiple leads.

## 1. Introduction

Despite their low cost and extreme versatility, modern semiconductor transistors face fundamental obstacles to continued miniaturization. First, top-down fabrication gives them microscopic variability from device to device, which, while acceptable at today's length scales, renders them unscalable in the nanometre regime. Second, these devices, like all field-effect devices, function by raising and lowering an energy barrier to charge transport of at least  $k_B T$ ; each device therefore dissipates energy of this magnitude into the environment with every switching cycle<sup>3</sup>. At device densities greater than the current state of the art, the cost and engineering challenges associated with removing the resultant heat are daunting [2]. While the first challenge can be met by utilizing the bottom-up chemical fabrication of single-molecule devices (e.g. [3]), this approach in itself does nothing to address the need for a cooler switching mechanism.

An alternative paradigm to raising and lowering an energy barrier is to exploit the wave nature of the electron to control the current flow [4–9]. Traditionally, such interference-based devices are modulated via the Aharonov–Bohm effect [10]. This, however, is incompatible with the small size of molecular devices [4]: through a  $1 \text{ nm}^2$  device, a magnetic field of over 600 T would be required to generate a phase shift of order 1 rad. Similarly, a device based on an electrostatic phase shift [7] would require voltages incompatible with structural stability. Previously [11], we have proposed a solution,

<sup>3</sup> This is to be distinguished from the heating due to irreversible computation of [1].

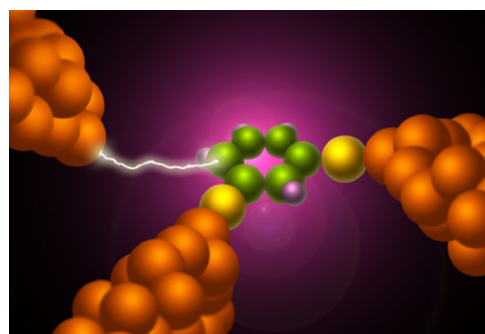


**Figure 1.** Artist's conception of a quantum interference effect transistor based on 1,3-benzenedithiol. The coloured spheres represent individual carbon (green), hydrogen (purple), sulfur (yellow), and gold (orange) atoms. In the 'off' state of the device, destructive interference blocks the flow of current between the source (bottom) and drain (right) electrodes. Decoherence introduced by the scanning transmission microscope (STM) tip (upper left) suppresses interference, allowing current flow. Image by Helen M Giesel.

called the quantum interference effect transistor (QuiET) (see figure 1), which exploits a perfect destructive interference due to molecular symmetry and controls quantum transport by introducing decoherence or elastic scattering.

The purpose of this article is to communicate the details of this proposal, including several potential chemical structures, to facilitate fabrication and testing of this device. In section 2, we describe the theoretical framework used to model the device. Section 3 explains the QuiET's operating mechanism.

Section 4 discusses practical implementations of the device. We conclude in section 5.

## 2. Theoretical model

The QuIET consists of a central molecular element, two leads chemically bonded to the molecule, and a third lead, which can be coupled to the molecule either capacitively or via tunnelling. The Hamiltonian of this system can be written as the sum of three terms:

$$H = H_{\text{mol}} + H_{\text{leads}} + H_{\text{tun}}. \quad (1)$$

The first is the  $\pi$ -electron molecular Hamiltonian

$$H_{\text{mol}} = \sum_{n\sigma} \varepsilon_n d_{n\sigma}^\dagger d_{n\sigma} - \sum_{nm\sigma} (t_{nm} d_{n\sigma}^\dagger d_{m\sigma} + \text{H.c.}) + \sum_{nm} \frac{U_{nm}}{2} Q_n Q_m, \quad (2)$$

where  $d_{n\sigma}^\dagger$  creates an electron of spin  $\sigma = \uparrow, \downarrow$  in the  $\pi$ -orbital of the  $n$ th carbon atom, and  $\varepsilon_n$  are the orbital energies. We use a tight-binding model for the hopping matrix elements with  $t_{nm} = 2.2, 2.6$  or  $2.4$  eV for orbitals connected by a single bond, double bond, or within an aromatic ring, respectively, and zero otherwise. The final term of equation (2) contains intrasite and intersite Coulomb interactions, as well as the electrostatic coupling to the leads. The interaction energies are given by the Ohno parameterization [15, 16]:

$$U_{nm} = \frac{11.13 \text{ eV}}{\sqrt{1 + .6117 (R_{nm}/\text{\AA})^2}}, \quad (3)$$

where  $R_{nm}$  is the distance between orbitals  $n$  and  $m$ .

$$Q_n = \sum_{\sigma} d_{n\sigma}^\dagger d_{n\sigma} - \sum_{\alpha} C_{n\alpha} \mathcal{V}_{\alpha} / e - 1 \quad (4)$$

is an effective charge operator [17] for orbital  $n$ , where the second term represents a polarization charge. Here  $C_{n\alpha}$  is the capacitance between orbital  $n$  and lead  $\alpha$ , chosen consistent with the interaction energies of equation (3) and the geometry of the device, and  $\mathcal{V}_{\alpha}$  is the voltage on lead  $\alpha$ .  $e$  is the magnitude of the electron charge.

Each metal lead  $\alpha$  possesses a continuum of states, and their total Hamiltonian is

$$H_{\text{leads}} = \sum_{\alpha=1}^3 \sum_{k\in\alpha}^{\sigma} \epsilon_k c_{k\sigma}^\dagger c_{k\sigma}, \quad (5)$$

where the  $\epsilon_k$  are the energies of the single-particle levels in the leads, and  $c_{k\sigma}^\dagger$  is an electron creation operator. Here leads 1 and 2 are the source and drain, respectively, and lead 3 is the control, or gate electrode.

Tunnelling between molecule and leads is provided by the final term of the Hamiltonian,

$$H_{\text{tun}} = \sum_{(n\alpha)} \sum_{k\in\alpha}^{\sigma} (V_{nk} d_{n\sigma}^\dagger c_{k\sigma} + \text{H.c.}), \quad (6)$$

where the  $V_{nk}$  are the tunnelling matrix elements from a level  $k$  within lead  $\alpha$  to the nearby  $\pi$ -orbital  $n$  of the molecule. Coupling of the leads to the molecule via molecular chains, as may be desirable for fabrication purposes, can be included

in the effective  $V_{nk}$ , as can the effect of substituents (e.g., thiol groups) used to bond the leads to the molecule [18, 19].

We use the non-equilibrium Green function (NEGF) approach [20, 21] to describe transport in this open quantum system. The retarded Green function of the full system is

$$G(E) = [E - H_{\text{mol}} - \Sigma(E)]^{-1}, \quad (7)$$

where  $\Sigma$  is an operator, known as the retarded self-energy, describing the coupling of the molecule to the leads. The QuIET is intended for use at room temperature, and it operates in a voltage regime where there are no unpaired electrons in the molecule. Thus lead–lead and lead–molecule correlations, such as the Kondo effect, do not play an important role. Electron–electron interactions may therefore be included via the self-consistent Hartree–Fock method.  $H_{\text{mol}}$  is replaced by the corresponding mean-field Hartree–Fock Hamiltonian  $H_{\text{mol}}^{\text{HF}}$ , which is quadratic in electron creation and annihilation operators, and contains long-range hopping. Within mean-field theory, the self-energy is a diagonal matrix

$$\Sigma_{n\sigma, m\sigma'}(E) = \delta_{nm} \delta_{\sigma\sigma'} \sum_{(\alpha\alpha')} \delta_{n\alpha} \Sigma_{\alpha}(E), \quad (8)$$

with nonzero entries on the  $\pi$ -orbitals adjacent to each lead  $\alpha$ :

$$\Sigma_{\alpha}(E) = \sum_{\substack{k\in\alpha \\ (n\alpha)}} \frac{|V_{nk}|^2}{E - \epsilon_k + i0^+}. \quad (9)$$

The imaginary parts of the self-energy matrix elements determine the Fermi's Golden Rule tunnelling widths

$$\Gamma_{\alpha}(E) \equiv -2\text{Im}\Sigma_{\alpha}(E) = 2\pi \sum_{k\in\alpha} |V_{nk}|^2 \delta(E - \epsilon_k). \quad (10)$$

As a consequence, the molecular density of states changes from a discrete spectrum of delta functions to a continuous, width-broadened distribution. We take the broad-band limit [20], treating the  $\Gamma_{\alpha}$  as constants characterizing the coupling of the leads to the molecule. Typical estimates [19] using the method of [22] yield  $\Gamma_{\alpha} \lesssim 0.5$  eV, but values as large as 1 eV have been suggested [18].

The effective hopping and orbital energies in  $H_{\text{mol}}^{\text{HF}}$  depend on the equal-time correlation functions, which are found in the NEGF approach to be

$$\langle d_{n\sigma}^\dagger d_{m\sigma} \rangle = \sum_{(\alpha\alpha')} \frac{\Gamma_{\alpha}}{2\pi} \int_{-\infty}^{\infty} dE G_{n\sigma, \alpha\sigma}(E) G_{\alpha\sigma, m\sigma}^*(E) f_{\alpha}(E), \quad (11)$$

where  $f_{\alpha}(E) = \{1 + \exp[(E - \mu_{\alpha})/k_B T]\}^{-1}$  is the Fermi function for lead  $\alpha$ . Finally, the Green function is determined by iterating the self-consistent loop, equations (7)–(11).

The current in lead  $\alpha$  is given by the multi-terminal current formula [23]

$$I_{\alpha} = \frac{2e}{h} \sum_{\beta=1}^3 \int_{-\infty}^{\infty} dE T_{\beta\alpha}(E) [f_{\beta}(E) - f_{\alpha}(E)], \quad (12)$$

where

$$T_{\beta\alpha}(E) = \Gamma_{\beta} \Gamma_{\alpha} |G_{b\alpha}(E)|^2 \quad (13)$$

is the transmission probability [21] from lead  $\alpha$  to lead  $\beta$ , and  $a$  ( $b$ ) is the orbital coupled to lead  $\alpha$  ( $\beta$ ). Similar mean-field NEGF calculations have been widely used to treat two-terminal transport through single molecules [13].

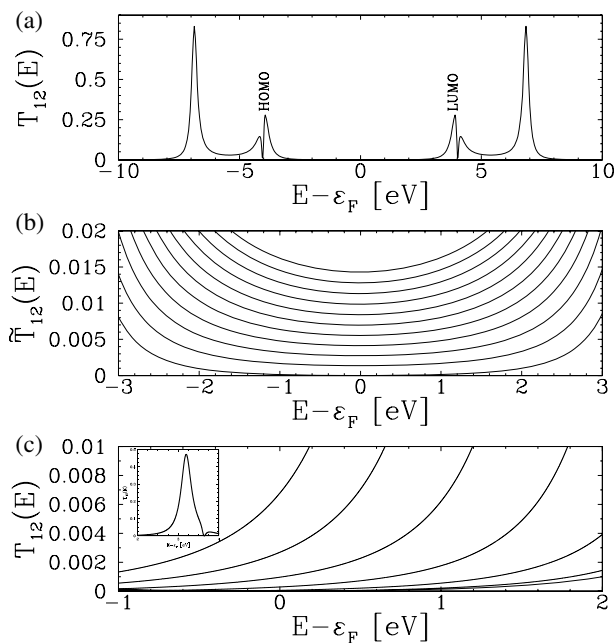


**Figure 2.** Effective transmission probability  $\tilde{T}_{12}$  of the device shown in figure 1, at room temperature, with  $\Gamma_1 = 1.2$  eV and  $\Gamma_2 = .48$  eV. Here  $\varepsilon_F$  is the Fermi level of the molecule. (a)  $\Sigma_3 = 0$ ; (b)  $\Sigma_3 = -i\Gamma_3/2$ , where  $\Gamma_3 = 0$  in the lowest curve, and increases by .24 eV in each successive one; (c)  $\Sigma_3$  is given by equation (15) with a single resonance at  $\varepsilon_v = \varepsilon_F + 4$  eV. Here  $t_\nu = 0$  in the lowest curve, and increases by 0.5 eV in each successive curve. Inset: full vertical scale for  $t_\nu = 1$  eV. Reprinted with permission from [11]. © 2006 American Chemical Society.

### 3. Switching mechanism

The QuIET exploits quantum interference stemming from the symmetry of monocyclic aromatic annulenes such as benzene. Quantum transport through single benzene molecules with two metallic leads connected at *para* positions has been the subject of extensive experimental and theoretical investigation [13]; however, a QuIET based on benzene requires the source (1) and drain (2) to be connected at *meta* positions, as illustrated in figure 1. The transmission probability  $T_{12}$  of this device, for  $\Sigma_3 = 0$ , is shown in figure 2. Due to the molecular symmetry [8], there is a node in  $T_{12}(E)$ , located midway between the highest occupied molecular orbital (HOMO) and lowest unoccupied molecular orbital (LUMO) energy levels (see figure 2(b), lowest curve). This mid-gap node, at the Fermi level of the molecule, plays an essential role in the operation of the QuIET.

The existence of a transmission node for the *meta* connection can be understood in terms of the Feynman path integral formulation of quantum mechanics [24], according to which an electron moving from lead 1 to lead 2 takes all possible paths within the molecule; observables relate only to the complex sum over paths. In the absence of a third lead ( $\Sigma_3 = 0$ ), these paths all lie within the benzene ring. An electron entering the molecule at the Fermi level has de Broglie wavevector  $k_F = \pi/2d$ , where  $d = 1.397$  Å is the intersite spacing of benzene (note that  $k_F$  is a purely geometrical quantity, which is unaltered by electron–electron interactions [25]). The two most direct paths through the ring

have lengths  $2d$  and  $4d$ , with a phase difference  $k_F 2d = \pi$ , so they interfere destructively. Similarly, all of the paths through the ring cancel exactly in a pairwise fashion, leading to a node in the transmission probability at  $E = \varepsilon_F$ .

This transmission node can be lifted by introducing decoherence or elastic scattering that breaks the molecular symmetry. Figures 2(b) and (c) illustrate the effect of coupling a third lead to the molecule, introducing a complex self-energy  $\Sigma_3(E)$  on the  $\pi$ -orbital adjacent to that connected to lead 1 or 2. An imaginary self-energy  $\Sigma_3 = -i\Gamma_3/2$  corresponds to coupling a third metallic lead directly to the benzene molecule, as shown in figure 1. If the third lead functions as an infinite-impedance voltage probe, the effective two-terminal transmission is [12]

$$\tilde{T}_{12} = T_{12} + \frac{T_{13}T_{32}}{T_{13} + T_{32}}. \quad (14)$$

The third lead introduces decoherence [12] and additional paths that are not cancelled, thus allowing current to flow, as shown in figure 2(b). This quantum-mechanical effect of the third lead is a fundamentally different switching mechanism from other proposed molecular transistors, such as [3], which rely on electrostatic gating to control the current. As a proof of principle, a QuIET could be constructed using a scanning tunnelling microscope (STM) tip as the third lead (cf figure 1), with tunnelling coupling  $\Gamma_3(x)$  to the appropriate  $\pi$ -orbital of the benzene ring, the control variable  $x$  being the piezo-voltage controlling the tip–molecule distance.

By contrast, a real self-energy  $\Sigma_3$  introduces elastic scattering, which can also break the molecular symmetry. This can be achieved by attaching a second molecule to the benzene ring, for example an alkene chain. The retarded self-energy due to the presence of a second molecule is

$$\Sigma_3(E) = \sum_\nu \frac{|t_\nu|^2}{E - \varepsilon_\nu + i0^+}, \quad (15)$$

where  $\varepsilon_\nu$  is the energy of the  $\nu$ th molecular orbital of the second molecule, and  $t_\nu$  is the hopping integral coupling this orbital with the neighbouring  $\pi$ -orbital of the benzene ring. Figure 2(c) shows the transmission probability  $T_{12}(E)$  in the vicinity of the Fermi energy of the molecule, for the case of a single side orbital at  $\varepsilon_\nu = \varepsilon_F + 4$  eV. As the coupling  $t_\nu$  is increased, the node in transmission at  $E = \varepsilon_F$  is lifted due to scattering from the side orbital. The side group introduces Fano antiresonances [5, 26], which suppress current through one arm of the annulene, thus lifting the destructive interference. Put another way, the second molecule's orbitals hybridize with those of the annulene, and a state that connects leads 1 and 2 is created in the gap (see figure 2(c) (inset)). In practice, either  $t_\nu$  or  $\varepsilon_\nu$  might be varied to control the strength of Fano scattering.

Tunable current suppression occurs over a broad energy range, as shown in figure 2(b); the QuIET functions with any metallic leads whose work function lies within the annulene gap. Fortunately, this is the case for many bulk metals, among them palladium, iridium, platinum, and gold [27]. Appropriately doped semiconductor electrodes [14] could also be used.

We show in figure 3 the  $I$ - $V$  characteristic of a QuIET based on sulfonated vinylbenzene. The three metallic

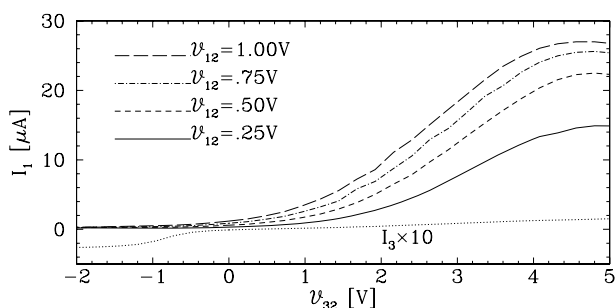


**Figure 3.** Room-temperature  $I$ - $V$  characteristic of a QuIET based on sulfonated vinylbenzene. The current in lead 1 is shown, where  $V_{\alpha\beta} = V_{\alpha} - V_{\beta}$ . Here,  $\Gamma_1 = \Gamma_2 = 1$  eV.  $\Gamma_3$  is taken as 0.0024 eV, which allows a small current in the third lead, so that the device amplifies current. A field-effect device with almost identical  $I$ - $V$  can be achieved by taking  $\Gamma_3 = 0$ . The curve for  $I_3$  is for the case of 1.00 V bias voltage;  $I_3$  for other biases look similar. Reprinted with permission from [11]. © 2006 American Chemical Society.

electrodes were taken as bulk gold, with  $\Gamma_1 = \Gamma_2 = 1$  eV, while  $\Gamma_3 = 0.0024$  eV, so that the coupling of the third electrode to the alkene side group is primarily electrostatic. The device characteristic resembles that of a macroscopic transistor. As the voltage on lead 3 is increased, scattering from the antibonding orbital of the alkene side group increases as it approaches the Fermi energies of leads 1 and 2, leading to a broad peak in the current. For  $\Gamma_{1,2} \gg \Gamma_3 \neq 0$ , the device amplifies the current in the third lead (dotted curve), emulating a bipolar junction transistor. Alkene chains containing four and six carbon atoms were also studied, yielding devices with characteristics similar to that shown in figure 3, with the maximum current  $I_1$  shifting to smaller values of  $V_{32}$  with increasing chain length. As evidence that the transistor behaviour shown in figure 3 is due to the tunable interference mechanism discussed above, we point out that if hopping between the benzene ring and the alkene side group is set to zero, so that the coupling of the side group to benzene is purely electrostatic, almost no current flows between leads 1 and 2.

For  $\Gamma_3 = 0$ ,  $I_3 = 0$  and the QuIET behaves as a field-effect transistor. The transconductance  $dI/dV_{32}$  of such a device is shown in figure 4. For comparison, we note that an ideal single-electron transistor [28] with  $\Gamma_1 = \Gamma_2 = 1$  eV has peak transconductance  $(1/17)G_0$  at bias voltage .25 V, and  $(1/2)G_0$  at bias 1 V, where  $G_0 = 2e^2/h$  is the conductance quantum. For low biases, the proposed QuIET thus has a higher transconductance than the prototypical nanoscale amplifier, while even for large biases its peak transconductance is comparable. Likewise, the load resistances required for a QuIET to have gain (load times transconductance) greater than one while in its 'on' state are comparable to other nanoscale devices,  $\sim 10/G_0$ .

Operation of the QuIET does not depend sensitively on the magnitude of the lead-molecule coupling  $\bar{\Gamma} = \Gamma_1\Gamma_2/(\Gamma_1 + \Gamma_2)$ . The current through the device decreases with decreasing  $\bar{\Gamma}$ , but aside from that, the device characteristic was found to be qualitatively similar when  $\bar{\Gamma}$  was varied over one order of magnitude. The QuIET is also insensitive to molecular vibrations: only vibrational modes that simultaneously alter the carbon-carbon bond lengths and break the six-fold symmetry within the benzene component can cause

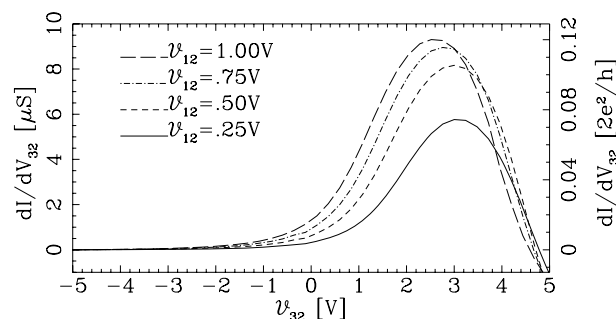


**Figure 4.** Transconductance  $dI/dV_{32}$  of a QuIET based on sulfonated vinylbenzene with  $\Gamma_3 = 0$ . The characteristic is similar to that of a field-effect transistor, i.e.  $I_3 = 0$  while  $I_1 = -I_2 = I$ . As in figure 3,  $\Gamma_1 = \Gamma_2 = 1$  eV, and the calculation was done for room temperature. Reprinted with permission from [11]. © 2006 American Chemical Society.

decoherence in a benzene 'interferometer'. Such modes are only excited at temperatures greater than about 500 K.

The position of the third lead affects the degree to which destructive interference is suppressed. For benzene, the most effective location for the third lead is shown in figure 1. It may also be placed at the site immediately between leads 1 and 2, but the transistor effect is somewhat reduced, since coupling to the charge carriers is less. The third, three-fold symmetric configuration of leads completely decouples the third lead from electrons travelling between the first two leads. For each monocyclic aromatic annulene, one three-fold symmetric lead configuration exists, yielding no transistor behaviour.

While  $H_{\text{mol}}$  of equation (2) is well known to reproduce the basic experimental features of conjugated molecules [29], the QuIET's characteristics, based on general principles of quantum mechanics and symmetry, are qualitatively independent of the particulars of the quantum chemical method. Inclusion of  $\sigma$  electrons, for example, has little effect: they form a separate system of localized bonds, and so cannot contribute strongly to transport. We have verified via an all-valence extended Hückel theory [30] that the QuIET's tunable coherent current suppression persists for such extensions of the basis set.

The QuIET's operating mechanism, tunable coherent current suppression, occurs over a broad energy range within the gap of each monocyclic aromatic annulene; it is thus a very robust effect, insensitive to moderate fluctuations of the electrical environment of the molecule. Although based on an entirely different, quantum-mechanical, switching mechanism, the QuIET nonetheless reproduces the functionality of macroscopic transistors on the scale of a single molecule. Furthermore, since the current flow is not blocked by an energy barrier, which must be raised and lowered with each switching cycle, heating of the environment is greatly reduced.

## 4. Implementations

As daunting as the fundamental problem of the switching mechanism is the practical one of nanofabrication. The QuIET requires a third lead coupled locally to the central molecule, and, while there has recently been significant progress in

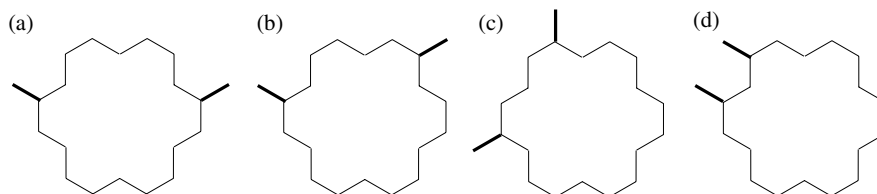


**Figure 5.** Source–drain lead configurations possible in a QuIET based on [18]annulene. The bold lines represent the positioning of the two leads. Each of the four arrangements has a different phase difference associated with it: (a)  $\pi$ ; (b)  $3\pi$ ; (c)  $5\pi$ ; and (d)  $7\pi$ . The slight deviations of [18]annulene's hydrogen atoms from the molecular plane do not significantly affect the QuIET's switching mechanism. Reprinted with permission from [11]. © 2006 American Chemical Society.

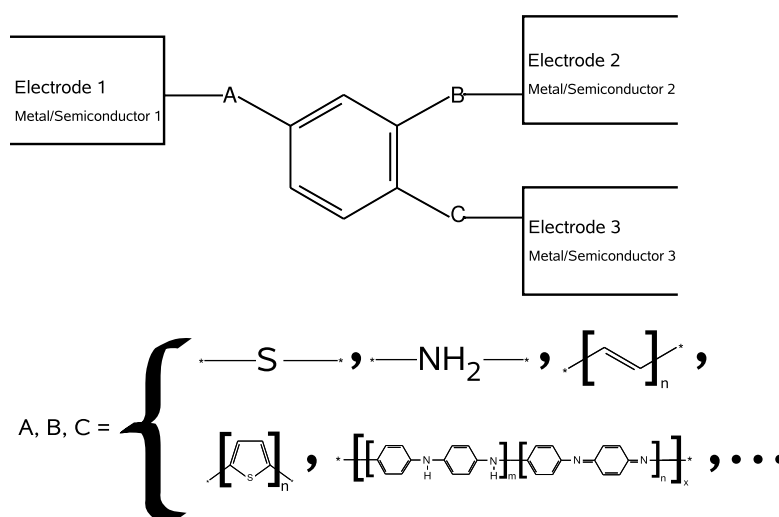


**Figure 6.** Schematic of various QuIETs based on a benzene ring. A, B, and C represent the various substituents which may be placed in series between the ring and each lead. In particular, the conducting polymers like polyaniline and polythiophene may be useful in overcoming the 'third lead' problem.

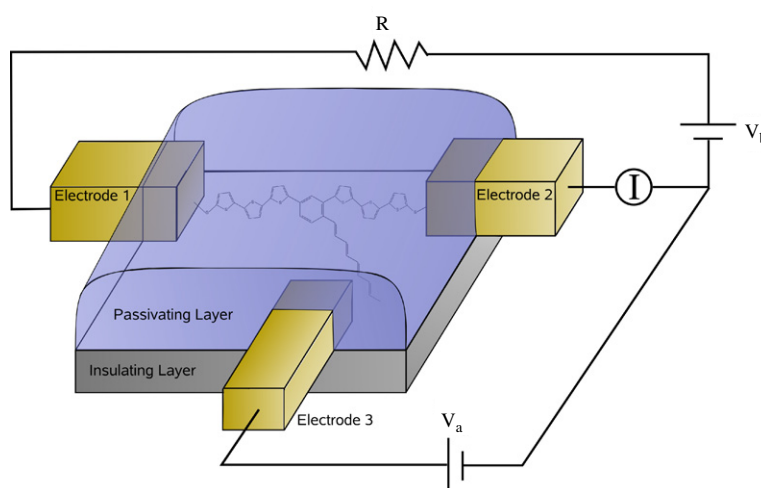


**Figure 7.** Possible embodiment of a QuIET integrated with conventional circuitry on a chip. The source (1) and drain (2) electrodes are connected via conducting polymers (in this case, polythiophene) to the central aromatic ring, while the gate electrode (3) is coupled electrostatically to an alkene side group.

(This figure is in colour only in the electronic version)

that direction [14, 31, 32], to date, only two-lead single-molecular devices, sometimes with global gating, have been achieved [13]. With this in mind, we turn to potential practical realizations of the device.

Using novel fabrication techniques, such as ultra-sharp STM tips [31] or substrate pitting [32], it may soon be possible to attach multiple leads to large molecules. Fortunately, the QuIET mechanism applies not only to benzene, but to any

monocyclic aromatic annulene with leads 1 and 2 positioned so the two most direct paths have a phase difference of  $\pi$ . Furthermore, larger molecules have other possible lead configurations, based on phase differences of  $3\pi$ ,  $5\pi$ , etc; as an example, figure 5 shows the lead configurations for a QuIET based on [18]annulene. Other large ring-like molecules that possess an aromatic conjugated electron system, such as [14]annulene and the divalent metal-phthalocyanines, would also serve well.

Another method of increasing the effective size of the molecule is to introduce molecular wires linking the central ring and leads (see figures 6 and 7). Conducting polymers, such as polythiophene or polyaniline, are ideal for this task. Such changes can be absorbed into the diagonal elements of the self-energy  $\Sigma(E)$ , and so only modify  $G(E)$  locally. As such, while they can significantly modify the on-resonance behaviour of a molecular device, the off-resonance function is largely unaltered. In particular, the transmission node at the centre of the gap is unaffected. An example of such a QuIET integrated with conventional circuitry on a chip is shown in figure 7.

## 5. Conclusions

The quantum interference effect transistor represents one way to simultaneously overcome the problems of scalability and power dissipation which face the next generation of transistors. Because of the exact symmetry possible in molecular devices, it possesses a perfect mid-gap transmission node, which serves as the off state for the device. Tunably introduced decoherence or elastic scattering can lift this quantum interference effect, with the result of current modulation. Furthermore, a vast variety of potential chemical structures possess the requisite symmetry, easing fabrication difficulties. In particular, molecular wires, such as conducting polymers, can be used to extend the molecule to arbitrary size.

## Acknowledgments

This work was supported in part by National Science Foundation Grant Nos PHY0210750, DMR0312028, and DMR0705163.

## References

- [1] Landauer R 1961 *IBM J. Res. Dev.* **5** 183
- [2] *International Technology Roadmap for Semiconductors*: 2006 Update <http://public.itrs.net>

- [3] Di Ventra M, Pantelides S T and Lang N D 2000 *Appl. Phys. Lett.* **76** 3448
- [4] Sautet P and Joachim C 1988 *Chem. Phys. Lett.* **153** 511
- [5] Sols F, Macucci M, Ravaioli U and Hess K 1989 *Appl. Phys. Lett.* **54** 350
- [6] Joachim C and Gimzewski J K 1997 *Chem. Phys. Lett.* **265** 353  
Joachim C, Gimzewski J K and Tang H 1998 *Phys. Rev. B* **58** 16407
- [7] Baer R and Neuhauser D 2002 *J. Am. Chem. Soc.* **124** 4200
- [8] Yaliraki S N and Ratner M A 2002 *Ann. New York Acad. Sci.* **960** 153
- [9] Stadler R, Forshaw M and Joachim C 2003 *Nanotechnology* **14** 138  
Stadler R, Ami S, Forshaw M and Joachim C 2003 *Nanotechnology* **14** 722
- [10] Washburn S and Webb R A 1986 *Adv. Phys.* **35** 375
- [11] Cardamone D M, Stafford C A and Mazumdar S 2006 *Nano Lett.* **6** 2422
- [12] Büttiker M 1988 *IBM J. Res. Dev.* **32** 63
- [13] Nitzan A and Ratner M A 2003 *Science* **300** 1384 and references therein
- [14] Piva P G, DiLabio G A, Pitters J L, Zikovsky J, Rezeq M, Dogel S, Hofer W A and Wolkow R A 2005 *Nature* **435** 658
- [15] Ohno K 1964 *Theor. Chim. Acta* **2** 219
- [16] Chandross M, Mazumdar S, Liess M, Lane P A, Vardeny Z V, Hamaguchi M and Yoshino K 1997 *Phys. Rev. B* **55** 1486
- [17] Stafford C A, Kotlyar R and Das Sarma S 1998 *Phys. Rev. B* **58** 7091
- [18] Tian W, Datta S, Hong S, Reifengerger R, Henderson J I and Kubiak C P 1998 *J. Chem. Phys.* **109** 2874
- [19] Nitzan A 2001 *Annu. Rev. Phys. Chem.* **52** 681
- [20] Jauho A-P, Wingreen N S and Meir Y 1994 *Phys. Rev. B* **50** 5528
- [21] Datta S 1995 *Electronic Transport in Mesoscopic Systems* (Cambridge: Cambridge University Press) pp 293–342
- [22] Mujica V, Kemp M and Ratner M A 1994 *J. Chem. Phys.* **101** 6849
- [23] Büttiker M 1986 *Phys. Rev. Lett.* **57** 1761
- [24] Feynman R P and Hibbs A R 1965 *Quantum Mechanics and Path Integrals* (New York: McGraw-Hill)
- [25] Luttinger J M 1960 *Phys. Rev.* **119** 1153
- [26] Clerk A A, Waintal X and Brouwer P W 2001 *Phys. Rev. Lett.* **86** 4636
- [27] Marder M P 2000 *Condensed Matter Physics* (New York: Wiley)
- [28] Kastner M A 1992 *Rev. Mod. Phys.* **64** 849
- [29] Salem L 1966 *The Molecular Orbital Theory of Conjugated Systems* (New York: Benjamin)
- [30] Hoffman R 1963 *J. Chem. Phys.* **39** 1397
- [31] Rezeq M, Pitters J and Wolkow R 2006 *J. Chem. Phys.* **124** 204716
- [32] Mativetsky J M, Burke S A, Fostner S and Grutter P 2007 *Small* **3** 818